Applied Catalysis B: Environmental 146 (2014) 138–146

Contents lists available at ScienceDirect

Applied Catalysis B: Environmental

journal homepage: www.elsevier.com/locate/apcatb

Total oxidation of toluene over noble metal based Ce, Fe and Ni doped titanium oxides

T. Barakat[a,*], V. Idakiev[b,**], R. Cousin[a], G.-S. Shao[c], Z.-Y. Yuan[c], T. Tabakova[b], S. Siffert[a,*]

[a] Université du Littoral Côte d'Opale, Unité de Chimie Environnemental et Interactions sur le Vivant E.A.4492, 145 avenue Maurice Schumann, 59140 Dunkerque, France
[b] Institute of Catalysis, Bulgarian Academy of Sciences, 1113 Sofia, Bulgaria
[c] Institute of New Catalytic Materials Science, College of Chemistry, Nankai University, 300071 Tianjin, China

ARTICLE INFO

Article history:
Received 16 November 2012
Received in revised form 22 May 2013
Accepted 24 May 2013
Available online 2 June 2013

Keywords:
VOC oxidation
Doping
Macro-mesoporous titania
Palladium
Gold
Ageing test

ABSTRACT

The catalytic oxidation of toluene over macro-mesoporous titania loaded with noble metals (Au, Pd) and doped with three different metal oxides has been investigated. Doping of titania proved to offer a better reducibility for titania and greater activity towards toluene total oxidation, with a decrease of approximately 80 °C in T_{50} values for 5 wt% ceria (5CeTi) and iron (5FeTi) doped titania. After gold loading, 5CeTi supported material demonstrated the highest performance in the removal of toluene, with a total selectivity for CO_2 and formation of traces of benzene. Since CeTi support (unloaded and noble metal loaded) proved to be the most effective material in the oxidation of toluene, an investigation of the effect of dopant content of this material has been conducted. Higher ceria content resulted in higher surface area values, higher noble metal–support interaction (observed in DR-UV–VIS results) and consequently a greater activity. Moreover, palladium loaded catalysts (T_{50} around 219 °C) proved to be the best performing ones in terms of catalytic behaviour. Consequently, Pd5CeTi was tested for its durability under low toluene conversion rates in order to determine its stability and possible structural changes under these conditions. Doping and noble metal loading offered a stable activity of the catalysts in the conversion of toluene at low temperatures and for a long period of time, even though changes in TiO_2 crystal sizes were detected. Carbonaceous compounds were formed onto the used catalyst and their quantity was investigated by DTA-TGA experiments

1. Introduction

Through industrial progress and increased transportation, volatile organic compounds (VOCs) have become a widespread problem in today's society, having detrimental effects on air quality and human health. Remediation strategies are thus essential for a more sustainable development. Being highly toxic compounds, VOCs should be eliminated through processes ensuring their transformation into benign products, limiting their risk on human health and the environment. An effective way of achieving this objective is complete catalytic oxidation of these compounds into H_2O and CO_2, using supported noble metals (e.g. Au, Pt and Pd) [1–8]. The supporting material plays an important role in enhancing the activity of the noble metal active phase deposited onto it. It offers a mechanical strength and higher surface areas thus influencing the efficiency of this active phase through many parameters such as support-active phase interactions and better metal dispersion. This influence has been witnessed by a decrease in T_{50} values, temperature at which 50% conversion of VOC is achieved, of multiple noble metal loaded oxide supports [8–11]. It has also been discussed that the activity of tested samples is enhanced when highly porous supports are employed, such as macro-mesoporous materials. The importance of such a hierarchical structure resides in the increasing accessibility of VOC molecules within a catalytic system it offers. Therefore, a reduction in the resistance to diffusion of these molecules in the structure and a greater contact between reactant and catalyst are achieved, thus improving the latter's efficiency towards VOC elimination. Researchers such as Idakiev et al. [12,13] proved that the use of macro-mesoporous TiO_2 and ZrO_2 supports ensures an important activity towards the removal of benzene. Hosseini et al. [11,14] also discussed the use of a hierarchically structured titania in the removal of toluene and saw that, compared to non-porous titania, the activity is improved by the presence of a highly porous structure. They also showed the presence of a high interaction between the support and the active phase, which played an important role in the increase of the catalytic performance. Doping oxide materials with low percentages of metal oxides has also been found to promote a catalytic support's

* Corresponding authors.
** Corresponding author.
E-mail addresses: vasko_54@yahoo.com (V. Idakiev), Stephane.Siffert@univ-littoral.fr (S. Siffert).

0926-3373/$ – see front matter © 2013 Elsevier B.V. All rights reserved.
http://dx.doi.org/10.1016/j.apcatb.2013.05.064

performance in VOC oxidation reaction. In fact, Machold et al. [15] investigated the activity of VO_x-TiO_2 samples in the partial oxidation of methylethylketone (MEK) and proved that the highest activity is observed for catalysts comprising titania supports with vanadium loadings of 4–6 wt%. In an earlier work, we also tested doping titania with low percentages of vanadia or niobia in the total oxidation of toluene [16]. We managed to prove the existence of a greater support-active phase interaction induced by the presence of these dopants. This interaction played a key role in enhancing the catalysts' performances in oxidation reactions.

In this work, a hierarchically structured titania support was doped with three different metal oxides (Me_xO_y = CeO_2, Fe_2O_3 or NiO). Gold and palladium were loaded onto these doped materials and all prepared catalysts were characterized and investigated in the total oxidation of toluene. The main objective of this work is to discuss the effect of doping of oxide supports as well as the influence of loading these materials with a noble metal based active phase on their catalytic performance towards the removal of VOC molecules.

2. Experimental

2.1. Support synthesis technique

Hierarchically porous Me_xO_y-doped titanium oxides (Me = Ce, Fe or Ni) were synthesized using the low-temperature hydrothermal treatment method [13]. Firstly, 3 g of Pluronic F127 copolymer used as a surfactant was added to a mixture of 10 mL of deionized water and 50 mL of ethanol at room temperature. A mass corresponding to 5 wt% and 0.5 wt% of Me-nitrate salts were then added to the previously prepared solution. The resulting mixture was intensively stirred for 3 h, and then 5 mL of tetrabutyl titanate were added dropwise. The solution was kept under slow stirring for 24 h after which the obtained mixture was sealed in a Teflon-lined autoclave and aged statically at 80 °C for 24 h. Product were then filtered, washed and dried at 60 °C. Removal of the surfactant was accomplished through Soxhlet extraction with ethanol for 30 h. Prepared supports will be marked as 5MeTi and 0.5MeTi. After the preparation process, materials were calcined at 400 °C (1 °C min^{-1}) for 4 h under air at a flow rate of 2 L h^{-1}.

2.2. Preparation of noble metal loaded catalysts

Gold-based catalysts were prepared using the deposition-precipitation technique in a "Contalab" laboratory reactor (Contraves AG, Switzerland) under complete control of the reaction parameters [17–19]. The theoretical gold loading yield on 5MeTi materials is 3 wt% and prepared catalysts are named Au5MeTi. The gold precursor ($HAuCl_4 \cdot 3H_2O$, ≥49% Au basis, Sigma–Aldrich) was suspended in deionized water and the pH value was set to 8 by adding a Na_2CO_3 solution. Materials were added to the solution and kept under stirring for 1 h at 60 °C. The resulting precipitate was then filtered and washed so as to remove Cl^- ions, and then samples were dried under vacuum at 80 °C.

Palladium catalysts were prepared via the wet impregnation technique [20–22]. Supports were stirred with aqueous solution of $Pd(NO_3)_2$ (Sigma–Aldrich) at a speed of 75 rounds/min for 1 h, then dried at 60 °C in a rotary evaporator. Resulting catalysts are loaded with 1.5 wt% Pd and will be named Pd5MeTi. All noble metal loaded samples were calcined in air at 400 °C (1 °C min^{-1}) for 4 h.

2.3. Characterization techniques

The gold content was analyzed by ICP/OES (Optical Emission Spectrometer with a source of excitation Inductively Coupled Plasma), using a Varian Vista MPX CCD apparatus.

X-Ray Diffraction (XRD) measurements used to determine structural characteristics of prepared catalysts were carried out on a Brüker AXS D8 Advance diffractometer equipped with a copper anode (λ = 1.5406 Å) and a LynxEye detector. The scattering intensities were measured over an angular range of $20° < 2\theta < 80°$ for all the samples with a step-size of $\Delta(2\theta) = 0.02$ and a count time of 4s per step. The diffraction patterns have been indexed by comparison with the ICDD files. The average crystallite size of titania particles was calculated using the Scherrer equation applied to the most intense and well-defined anatase phase peak seen at $2\theta = 25.3°$.

Pore diameters and volumes were determined by N_2 adsorption–desorption isotherms collected at liquid nitrogen temperature using a Quantachrome NOVA 2000e sorption analyzer. The specific surface areas of the samples were calculated using the Brunauer–Emmett–Teller (BET) method. The pore-size distributions were determined from the adsorption branch of the isotherms using the Barett–Joyner–Halenda (BJH) method. Before carrying out measurements, each sample was degassed at 200 °C for more than 6 h.

Transmission Electron Microscopy (TEM) analysis was performed on a Philips Tecnai G20 microscope, operating at 200 kV in order to determine gold particle size in used catalysts. Samples were dispersed in ethanol and treated with ultrasound waves for 5 min, and then deposited on a copper grid coated with a preformed holey carbon film.

Temperature Programmed Reduction (TPR) experiments were carried out in an Altamira AMI-200 apparatus as to analyze the catalysts redox properties. The TPR profiles were obtained by passing flowing 5% H_2/Ar (30 mL min^{-1}) through the calcined sample (about 100 mg). The temperature was increased from room temperature to 900 °C at a rate of 5 °C min^{-1} whereas in sub-ambient tests (used for palladium loaded catalysts) the temperature was increased from −40 to 500 °C at a rate of 5 °C min^{-1}. The hydrogen concentration in the effluent was continuously monitored by a thermoconductivity detector (TCD).

Diffuse-reflectance (DR) UV/Vis spectra were recorded with a CARY 5000 (Varian) spectrophotometer in the spectral range of 200–800 nm.

The activity of each catalyst (100 mg) was determined by measuring the conversion of toluene (1000 ppm, ≥99.9%, Sigma–Aldrich) in flowing air (flow rate = 100 mL min^{-1}) using a Varian CP4900 Gas Micro-Chromatography. The oxidation reaction was carried out in a fixed-bed microreactor operating between 25 and 400 °C (1 °C min^{-1}). Prior to the oxidation reactions the catalysts were calcined at 400 °C (1 °C min^{-1}) in flowing air (2 L h^{-1}).

3. Results and discussion

XRD patterns of unloaded and gold loaded doped titania supports are presented in Fig. 1a and b. These patterns show well-defined peaks related to the anatase phase of the support (ICDD 89-4921). This indicates a good crystallization of these materials after thermal treatment at 400 °C. However, XRD patterns of 5NiTi sample show the existence of narrower anatase phase peaks (Fig. 1a). This can be attributed to a more pronounced crystallization of this solid. The BET surface area value of 5NiTi support also shows a good crystallization of this material, being the lowest compared to the other samples' values (5CeTi and 5FeTi). Out of all doped supports, 5CeTi sample shows the highest BET surface area and the lowest crystal size values (Table 1). This sample also presents the highest pore volume, even when compared to the undoped macro-mesoporous titania support. These results may indicate a possible rearrangement of TiO_2 crystals during thermal treatment and after doping of titania with Ce, thus creating a greater number of pore, and consequently providing a higher surface area value. It was also noted that pore diameter values increased after doping

Table 1
Structural characteristics of metal oxide doped macro-mesoporous titania supports and their corresponding gold loaded catalysts.

Samples	BET surface area ($m^2\ g^{-1}$)	TiO_2 crystal size (nm)[a]	D_{av} (nm)[b]	V_{pore} (cm^3/g)	Au wt% (Au particle size[c]; nm)	T_{50} (°C)
5FeTi	115	8.3	8.2	0.20	–	321
Au5FeTi	107	8.7	7.6	0.19	2.87	318
5NiTi	91	13.8	11.2	0.20	–	391
Au5NiTi	84	13.8	10.2	0.19	2.99	354
5CeTi	157	7.8	11.0	0.39	–	321
Au5CeTi	146	8.4	10.5	0.37	2.36 (9 nm)	297
Pd5CeTi	176	7.9	–	–	–	220
0.5CeTi	120	10.5	10.3	0.25	–	359
Au0.5CeTi	104	10.5	9.0	0.24	2.38 (6 nm)	312
Pd0.5CeTi	131	10.7	–	–	–	217
TiO_2	168	11.7	4.4	0.22	–	400

[a] Calculated using the Scherrer equation applied to XRD patterns.
[b] Pore average diameter.
[c] Gold particle sizes determined by TEM experiments.

of titania. We also detected the presence of peaks related to hematite ($2\theta = 30.7°$, 36.1° and 42.3°, ICDD 33-0664) and magnetite ($2\theta = 33.5°$, 35.6° and 40°, ICDD 89-0950) phases, as well as NiO ($2\theta = 37.3°$, ICDD 89-5881). Whereas in the case of 5CeTi, no peaks related to ceria species were detected. This can indicate that Ce species are incorporated into the matrix of the support and might be surrounded by Ti atoms. After gold loading, peaks related to metallic gold particles are seen at $2\theta = 44.4°$, 64.6° and 78.6° (ICDD 65-2870, Fig. 1b). When calculated using the Scherrer equation, we noticed that the size of these particles varies between 9 and 14 nm. The lowest Au crystallite size was detected in Au5CeTi, around 9.2 nm, which was verified by TEM images presented in Fig. 2.

In order to understand the behaviour of the catalysts in reductive processes, TPR experiments were conducted, and results are shown in Fig. 3(a, b, c and d). Profiles seen in Fig. 3 show the hydrogen consumption related to reduced species (dopants or noble metals), versus temperature. These consumptions are compared to theoretical ones calculated using the amount of particles introduced into the support during the synthesis of doped materials (Table 2). It is important to note that iron oxide (Fe_2O_3) and nickel oxide (NiO) are reduced to their metallic state whereas ceria is reduced from Ce(IV) to Ce(III). First of all we notice a small reduction peak on the titania TPR profile between 400 and 650 °C correlated with a partial reduction of TiO_2 (Fig. 3a). The beginning of another reduction peak seen at temperatures higher than 700 °C is related to a further reduction of the titania support [23]. As for 5CeTi, a low intensity reduction peak seen between 400 and 800 °C could be related to the reduction of Ce(IV) to Ce(III). The lower consumption of H_2 compared to the theoretical value indicates that not all

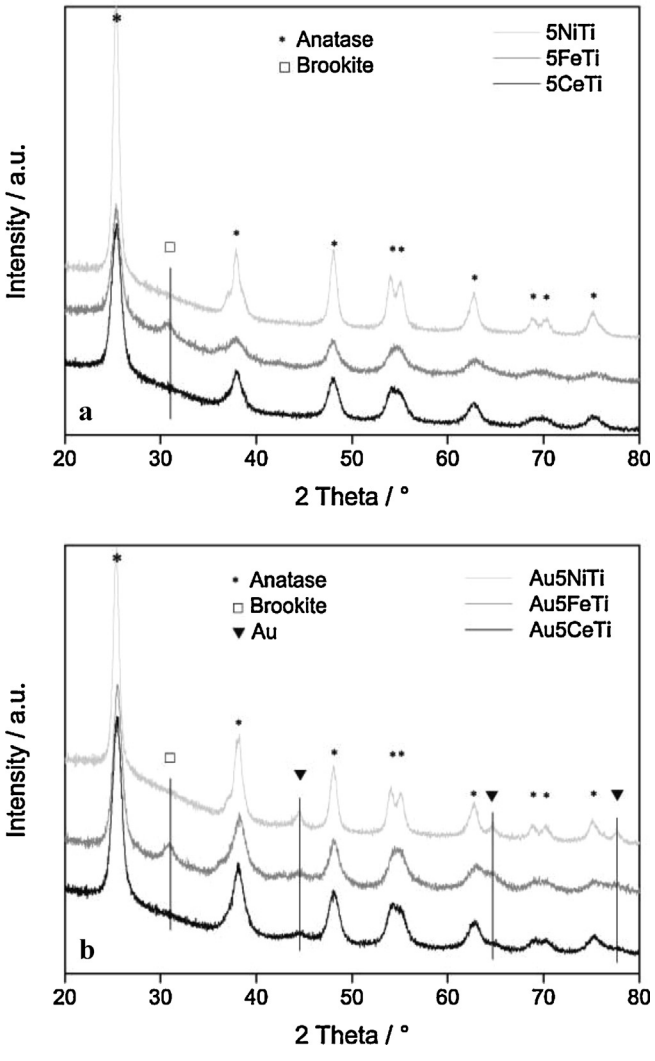

Fig. 1. XRD profiles of (a) doped titania supports and (b) their corresponding gold loaded catalysts.

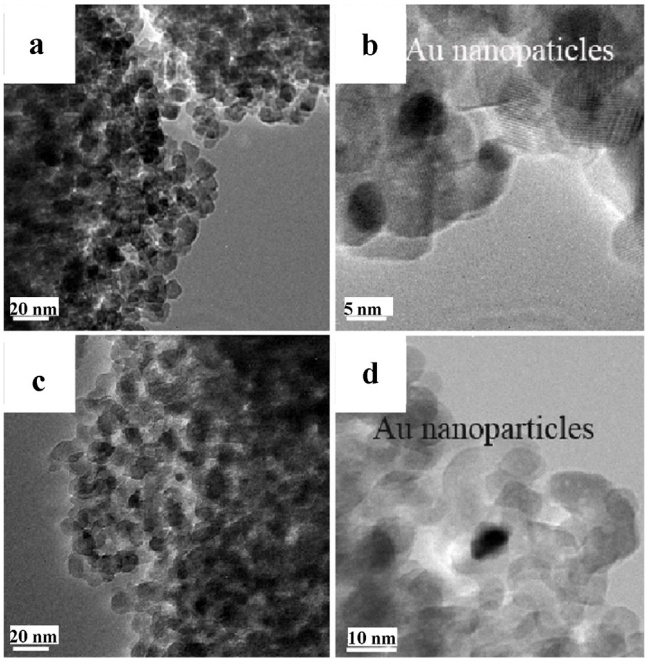

Fig. 2. TEM photos of 0.5CeTi (a), Au0.5 CeTi (b), 5CeTi (c) and Au5CeTi (d) catalysts.

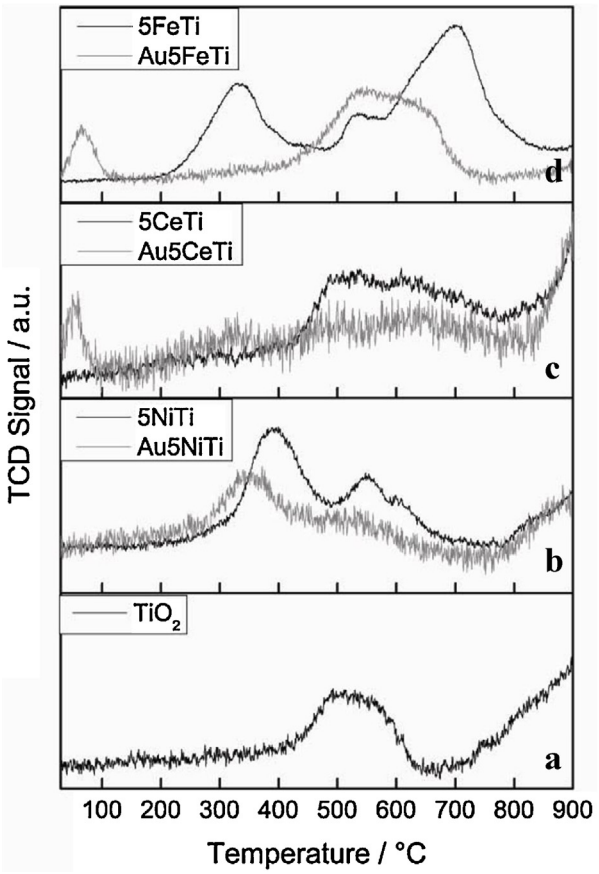

Fig. 3. TPR profiles of doped supports and their corresponding gold loaded catalysts.

ceria species have been reduced (Fig. 3c, Table 2). Zhu et al. [24] observed a low reduction peak at 510 °C for a mixed Ce-Ti support attributed to the reduction of the surface-capping oxygen of ceria. This discussion could suggest that the amount of ceria surface oxygen is lower in our 5CeTi support compared to results in the literature. This interpretation combined with the XRD results presented earlier could indicate that Ce particles are well incorporated into the TiO_2 matrix (as interpreted in XRD patterns). 5FeTi profile shows intense reduction peaks related to the reduction of hematite (T = 331 °C) and magnetite (T = 702 °C) (Fig. 3d) [25]. The H_2 over-consumption noted for this material can be related to a partial reduction of the titania support. As for 5NiTi, the spotted peaks can be assigned to the reduction of surface Ni(II) and nickel species present in the structure of the support, to metallic Ni (Fig. 3b). The low hydrogen consumption of this support can suggest the doping titania with nickel increases the resistance of the obtained material towards a reductive process.

After gold loading, experimental H_2 consumption values show a lower reduction of materials compared to values before gold loading. This can suggest that loaded gold particles protect their supported materials towards a reductive process (Table 2) [7,11]. Considering that all gold particles exist under their third oxidized state Au(III), when exposed to a reductive process, theoretical H_2 consumptions specific to the reduction of these species to metallic particles are calculated using the amount of loaded Au particles onto each support. Table 2 also shows that a part of Au particles exists already in its metallic state. This was verified by the low intensity of gold reduction peaks (seen at T < 100 °C) or their absence in the case of Au5NiTi. In order to verify this interpretation, UV–Visible experiments were conducted, and obtained results are shown in Fig. 4(a, b and c). The absorption band situated between 200 and 400 nm corresponds to a d-d electronic transition between a Ti^{4+} ion and an O^{2-} ligand. The higher intensity of this band seen in the spectra of unloaded doped supports can be correlated with the existence a greater number of Ti^{4+} ions and consequently, a greater number of Ti^{4+}-O^{2-} bonds. However, after gold loading, the intensity of this band decreased of approximately 0.9 absorbance units compared to that of unloaded doped supports. This can be due to the existence of an interaction between Au particles and the supported material [26]. A low intensity absorption band seen in the 5FeTi spectrum can be related to the presence of iron particles. The absorption band appearing between 500 and 700 nm after gold loading corresponds to the surface plasmon resonance of metallic Au nanoparticles [27]. The presence of this band depicts that gold exists in metallic state, which is in accordance with TPR results interpreted earlier. All samples were then tested in the oxidation of toluene as to compare their performances in the removal of VOC molecules.

Fig. 5 shows toluene conversion curves into CO_2 over unloaded and gold loaded catalysts between 100 and 400 °C, and T_{50} values (temperature at which 50% conversion of toluene is achieved) of each catalyst are presented in Table 1. Toluene conversion into CO_2 was calculated using the following equation:

Equation of toluene conversion into CO_2:

$$\text{Conv} = 100 \times \frac{[CO_{2(\text{formed})}]}{[CO_{2(\text{formed})}] + [CO_{(\text{formed})}] + 7 \times [\text{Toluene}_{(\text{remaining})}] + 6 \times [\text{Benzene}_{(\text{formed})}]}$$

First of all, it is clear that doping a macro-mesoporous titania provides an increase in this material's performance towards toluene total oxidation. After doping, T_{50} values decreased by 79 °C for both 5FeTi and 5CeTi (T_{50} = 321 °C) materials, and by 9 °C for 5NiTi. CO_2 and H_2O are the major products of the reaction. However, non-negligible quantities of CO and benzene were formed before reaching a 100% conversion rate. Furthermore, 5NiTi showed a low activity in toluene removal, reaching only 63% of toluene conversion at 400 °C. After gold loading, the activity increases even more, and the order of catalytic performance becomes the following: Au5CeTi > Au5FeTi = 5CeTi = 5FeTi > Au5NiTi > 5NiTi > TiO_2. It is also noted that gold loading of doped supports has provided 100% selectivity for CO_2, while traces of benzene are also detected before reaching 100% conversion of toluene (Table 3). In fact, at around 95% conversion, the only persisting VOC is toluene as benzene molecules oxidize to produce CO_2. Hosseini et al. [28] investigated the activity of a gold loaded macro-mesoporous titania in the total oxidation of toluene and observed that the T_{50} value related to this catalyst is approximately 340 °C. When compared to our results, 5CeTi and 5FeTi catalysts used in this work showed a significantly higher activity than the Au/undoped-TiO_2 catalyst, even before gold loading [28]. This clearly shows the beneficial effect of doping on the activity of TiO_2 and also on the activity of the obtained support after gold loading. A small decrease in surface areas after catalytic testing is observed and might be caused by the deposition of carbonaceous compounds formed during the oxidation reaction. This phenomenon will be closely studied further in this work. Finally, it is clear that Au5CeTi presented the best performance in the total oxidation of toluene. Moreover, 5CeTi support showed a similar activity to that of 5FeTi and Au5FeTi, meaning it was as active as a gold loaded doped catalyst. Based on these results and in order to study the effect of dopant yields on the activity of an oxide catalyst, ceria content was varied in CeTi supported materials and the resulting catalysts were tested in the oxidation of toluene.

TEM images of 0.5CeTi and 5CeTi supports and their corresponding gold loaded catalysts are reported in Fig. 2. EDX experiments showed that dark spots seen in Fig. 2 (a, and e) are related to the

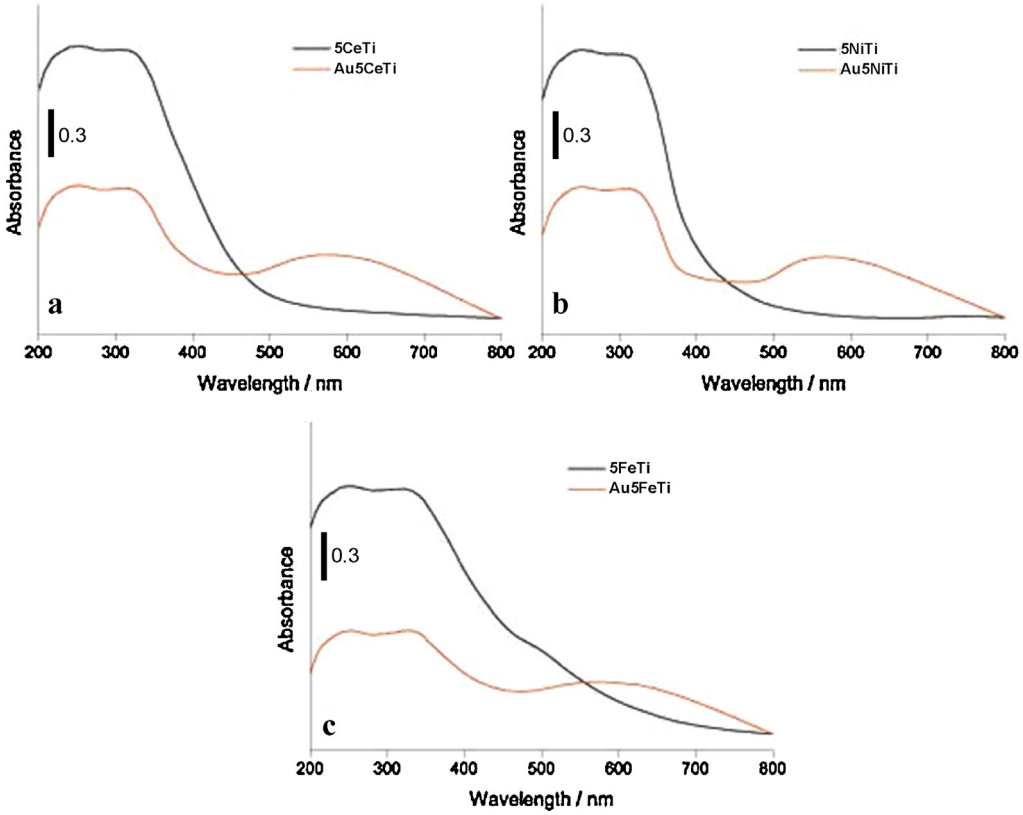

Fig. 4. DR-UV–Visible spectra of unloaded and gold loaded doped titania samples.

existence of ceria particles whereas darker spots seen in Fig. 2 (d and h) are associated with the presence of metallic gold particles deposited onto the support, and of 5 to 10 nm in size. The latter values are in accordance with gold crystal size values calculated using Scherrer's equation applied to gold specific XRD peak. Structural characteristics of 0.5 wt% and 5 wt% Ce doped titania materials and their corresponding noble metal loaded catalysts are reported in Table 1. The data shows that 0.5CeTi support possesses a lower BET surface area than 5CeTi. They also show lower pore volume values and a greater size for TiO_2 crystallites in 0.5CeTi. We also noticed that after palladium impregnation, both supports showed higher BET surface area values. XRD patterns of palladium loaded CeTi supports show an intense peak at $2\theta = 33.7^\circ$ (ICDD 85-0624) related to the existence of PdO particles. UV–Visible experiments were conducted on these catalysts and are reported in Fig. 6. As noted before, after noble metal loading, there was a decrease in the intensity of the anatase phase specific absorption band, depicting the presence of a noble metal–support interaction. The spectrum of Pd0.5CeTi exhibits an absorption band between 400 and 500 nm expected for PdO species [29], thus verifying XRD results. However, the profile of Pd5CeTi catalyst showed no absorption bands related to PdO species, thus suggesting the presence of small Pd particles compared, and in other words, a higher dispersion of Pd particles. Only a different content in ceria differentiates both catalysts. Therefore, it is clear, once more, that a support-noble metal interaction exists; in this case, ceria could have favoured Pd dispersion at the surface of the catalyst. The surface plasmon resonance band of metallic gold nanoparticles is observed for gold loaded samples, suggesting that gold exists in metallic state [27]. TPR experiments were then conducted in order to strengthen these interpretations. Ambient (a, b) and sub-ambient (c) TPR profiles of unloaded and noble metal loaded CeTi supports are reported in Fig. 7. After loading gold, the intensities of the support's reduction peaks decreased (Fig. 7a and b). This phenomenon can be correlated with an increase in the resistance of the support towards a reductive process [11]. Profiles for both palladium loaded catalysts show an intense reduction peak at $-10\,^\circ$C correlated with the reduction of surface PdO particles (Fig. 7c) [9,30]. Hydrogen consumption values calculated for this peak suggest that all Pd species are deposited at the surface of used materials (Table 4). The negative peak seen at around 100 °C is correlated with the decomposition of PdH_x hydrides formed at low temperatures [30,31]. It depicts that the reduction of PdO species

Table 2
Theoretical and experimental hydrogen consumption values of unloaded and gold loaded catalysts in TPR experiments.

Samples	H_2 theoretical consumption (μmol g^{-1})	H_2 experimental consumption (μmol g^{-1}) (corresponding temperature)				
	Dopants	Au	1st peak	2nd peak	3rd peak	Total
5FeTi	1342.9	–	616.8 (332 °C)	270.0 (532 °C)	1212.4 (701 °C)	2099.2
Au5FeTi	1342.9	218.6	124.0 (66 °C)	915.1 (373–763 °C)	–	1039.1
5CeTi	320.3	–	242.9 (422–780 °C)	–	–	242.9
Au5CeTi	320.3	179.7	42.1 (56 °C)	74.3 (332 °C)	198.1 (408–750 °C)	314.5
5NiTi	851.8	–	251.9 (390 °C)	107.3 (552 °C)	46.5 (602 °C)	405.7
Au5NiTi	851.8	227.7	180.3 (355 °C)	73.4 (534–740 °C)	–	253.7
TiO_2	–	–	124.4 (426–631 °C)	–	–	124.4

Table 3
Selectivity of unloaded and noble metal-loaded TiO_2 towards the formation of reaction products between 5 and 95% and at 100% conversion rate.

Sample/Selectivity	Unloaded TiO_2			Noble metal-loaded TiO_2			
	5FeTi	5CeTi	5NiTi	Au5FeTi	Au5CeTi Au0.5CeTi	Au5NiTi	Pd5CeTi Pd0.5CeTi
Reaction products formed between 5 and 95% conversion	CO_2 and H_2O presence of CO (0–400 ppm) and benzene (0–150 ppm)			CO_2 and H_2O presence of benzene (<20 ppm)			
Reaction products formed at 100% conversion	100% of CO_2 and H_2O			100% of CO_2 and H_2O			

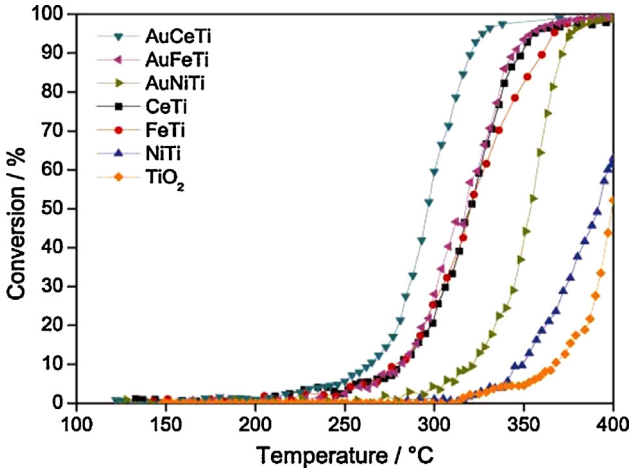

Fig. 5. Toluene conversion curves over unloaded and gold loaded Ce, Fe and Ni doped titania.

has already occurred. The absence of reduction peaks at higher temperatures can show that, in fact, palladium species are deposited at the surface of the support. It can also suggest that Pd particles form a protective layer around the support, thus causing a higher resistance towards reductive processes. Finally, the greater resistance of the supports towards a reductive process after noble metal loading might explain the influence of the noble metal–support interaction seen in UV–Visible spectra presented earlier (Fig. 6).

Samples were then subjected to catalytic testing in the total oxidation of toluene as means to understand the influence of phenomena seen through characterization techniques on the performance of tested catalysts. Light-off curves representing the conversion of toluene into CO_2 are presented in Fig. 8. A first comparison between catalytic performances of used catalysts shows that 5CeTi support presents a higher activity towards toluene oxidation than its counterpart 0.5CeTi. The same order of performance was noted for gold loaded catalysts, but activities of these catalysts were higher than those of unloaded doped supports. Palladium loaded catalysts offered similar activities, with T_{50} values decreasing by at least 70 °C compared to Au5CeTi, and approximately 100 °C compared to 5CeTi support. H_2-chemisorption results showed that Pd particles in Pd0.5CeTi are much larger (19.6 nm) than their counterparts in Pd5CeTi (8.9 nm). These results are consistent with those observed in UV–VIS experiments and can prove that a higher presence of Ce species increases Pd particle sizes while however maintaining a similar activity. Activity results of 0.5CeTi and 5CeTi materials and their corresponding noble metal based catalysts were compared to a previously studied 1.5PdTi sample [11]. Considering that T_{50} of the latter sample being approximately 226 °C, we can conclude that doping of macro-mesoporous titania offers indeed a beneficial effect in the oxidation of toluene in terms of catalytic activity. After noble metal loading, we always noted 100% selectivity for CO_2 and the formation of traces of benzene. A small decrease in surface area values for spent catalysts was also noted. This decrease can be due to the deposition of carbonaceous compounds. Such compounds were denoted as main causes for the deactivation of catalytic systems [32–34].

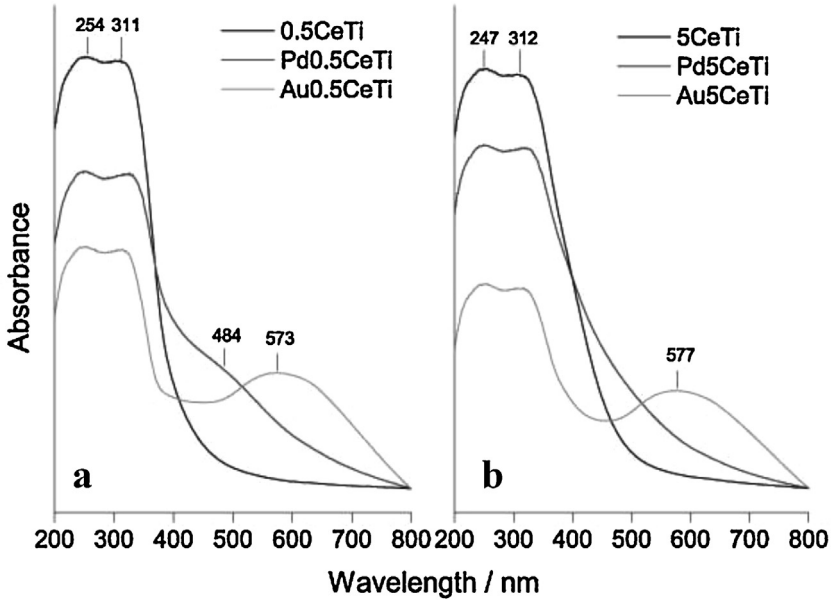

Fig. 6. DR-UV–Visible spectra of unloaded and noble metal loaded 0.5CeTi and 5CeTi materials.

Table 4
Theoretical and experimental hydrogen consumption values of palladium loaded CeTi supports in TPR experiments.

Samples	H_2 theoretical consumption (μmol g^{-1})	H_2 experimental consumption (μmol g^{-1}) (corresponding temperature)			
	Dopants	Pd	1st peak	negative peak	Total
Pd0.5CeTi	32.03	135.3	149.6 (−14 °C)	−15.5 (100 °C)	134.1
Pd5CeTi	320.3	130.6	160 (−10 °C)	−32.8 (100 °C)	127.2

Based on this fact, we exposed the best performing catalyst, Pd5CeTi, to 100 h of air and toluene (1000 ppm) at low conversion rates (15% conversion to CO_2, T = 213 °C) and under the same classical testing conditions. In fact, at 15% conversion rate, the deactivation process can be observed, far better than that seen at 100% conversion rate [28,35]. This deactivation can be caused by the formation and deposition of greater amounts of carbonaceous compounds at this low conversion rate. After testing, the sample was analyzed by different characterization techniques in order to determine any changes occurring in it. Ageing test results are shown in Fig. 9. A steep decrease in the activity of the sample (from nearly 16 to 10% conversion rates) was observed at t < 70 h, followed by a lesser decrease between 8 and 10% at t > 70 h depicting the beginning of a possible stabilization period. BET surface area measurements of the spent catalyst showed a decrease in surface area values from 176 to 159 m^2 g^{-1}. XRD patterns of the spent sample revealed a shifting of the anatase phase specific XRD peaks (ICDD 89-4921) to higher diffraction angles (for example from 25.3° to 26.3° for the most intense peak) which can suggest a possible change in the lattice parameters of this catalyst. We also observed the appearance of a new peak at 2θ = 40.6° attributed to the presence of metallic palladium crystallites (ICDD 87-0638). In fact, during the course of a VOC oxidation reaction, Pd^{2+} is reduced to metallic Pd while oxidizing the VOC, then metallic Pd particles tend to re-oxidize through a simple contact with oxygen species with decreasing temperatures, as discussed by Veser et al. [36] and McCarty [37]. Therefore, a greater site competition between oxygen and VOC molecules is observed on the catalyst's surface, thus creating a cycle-like activity for palladium particles. However, at the end of the reaction and after a high time-on-stream, palladium tends to exist mainly under its metallic state. Since during the deactivation reaction the catalyst was exposed to 100 h of constant flow of a toluene–air mixture, a possible deposition of carbonaceous compounds was suspected. Furthermore, TiO_2 crystal size value calculated using XRD patterns of the spent sample slightly increased compared to that of the fresh sample (7.9 to 8.1 nm at 2θ = 25.3°). This result might prove a possible resistance of the sample towards changes caused by the deposition of carbonaceous compounds or the exposition to great quantities of VOCs, which might explain the stabilization of the catalyst's activity after 70 h.

In order to verify the presence of carbonaceous compounds onto the surface of the catalyst, DTA-TGA experiments were conducted after the ageing test. These experiments revealed the existence of an endothermic peak at T < 150 °C followed by a 1.58% mass loss correlated with water molecules desorption from the catalyst, and two exothermic peaks at 202 °C and 286 °C followed by a mass loss of 1.03 and 7.44% respectively (Fig. 10). Dégé et al. [38] noticed the formation of coke after the combustion of xylene onto a Pd/HFAU catalyst and its combustion at approximately 400 °C. They argued that that coke formation can be related to the acidic properties of a catalyst. Tidahy et al. [39] also observed the deposition of carbonaceous compounds after toluene oxidation over different Pd loaded zeolites through EPR and DTA-TGA experiments and concluded

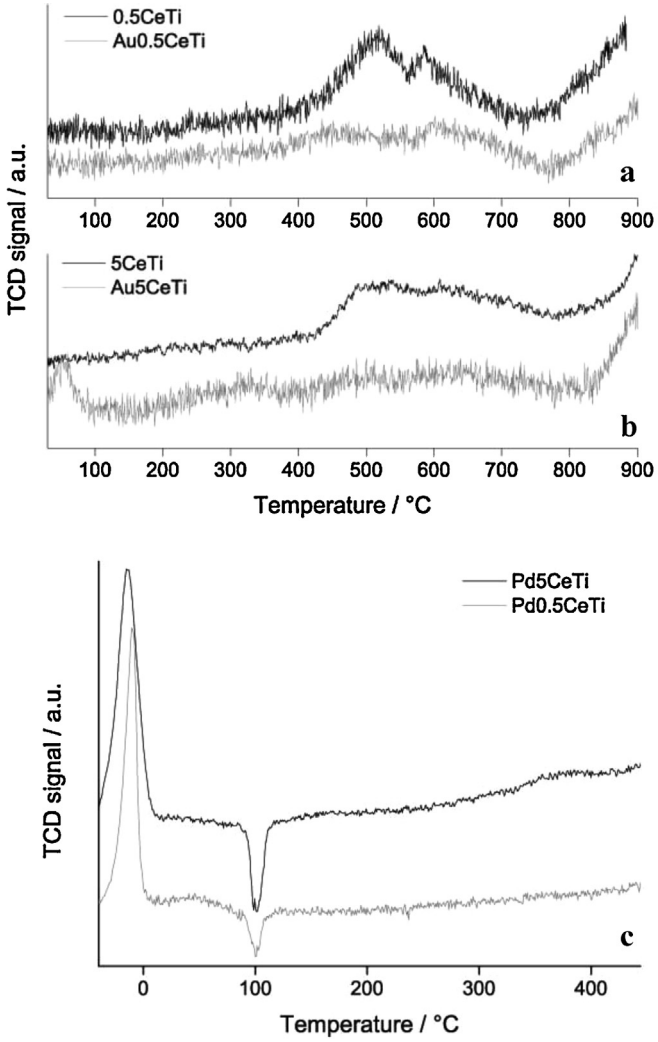

Fig. 7. TPR profiles of 0.5CeTi and 5CeTi and their corresponding gold and palladium loaded catalysts.

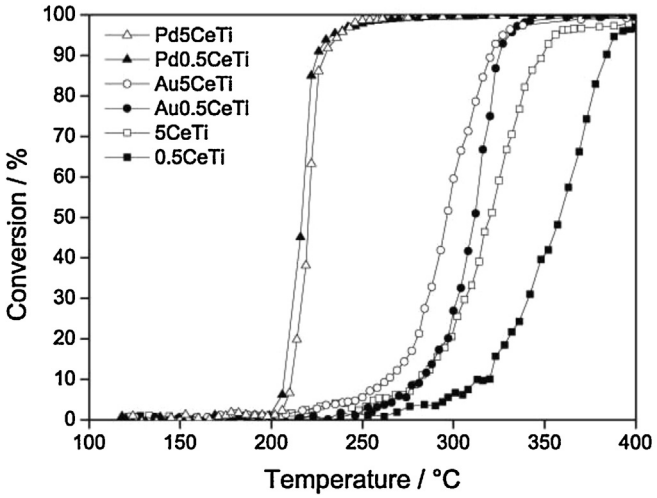

Fig. 8. Toluene conversion curves over unloaded and noble metal loaded 0.5 and 5CeTi catalysts.

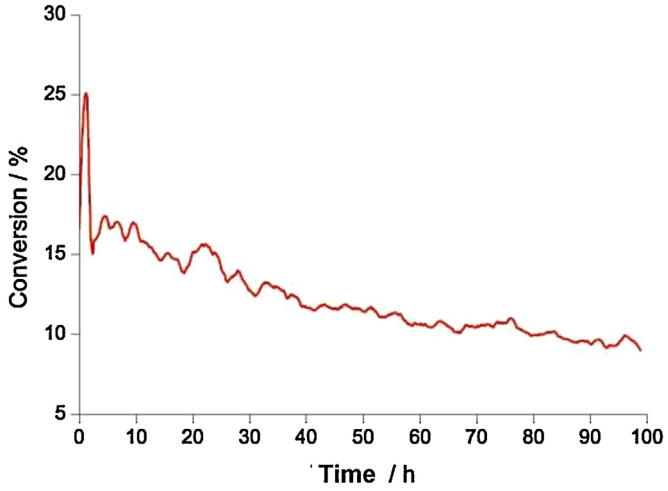

Fig. 9. Toluene conversion rate versus temperature in Pd5CeTi catalyst ageing test.

that higher loading amounts of coke can be caused by either acid properties or low activity of a support. Furthermore, Caeiro et al. [40] studied the deactivation of H-USY zeolites by coke molecules formed by the transformation of methylcyclohexane using the FTIR technique. They observed the presence of 2 types of coke molecules which they denoted as "light coke" (monoaromatic polysubstituted compounds) and "hard coke" (polyaromatic compounds). Hosseini et al. [11] also discussed the presence of these two types of coke molecules on noble metal loaded titania supports through DTA-TGA experiments. They observed two exothermic peaks at 325 °C and 525 °C which they related to light and hard coke respectively. Based on these results, the first peak at 202 °C was attributed to the removal of lightly adsorbed aromatic molecules. The second peak seen at 286 °C was attributed to the removal of highly adsorbed molecules, possibly created by the bonding of multiple fragments formed by the degradation of toluene. However, when compared to results discussed by Hosseini et al., we noticed a shifting of the exothermic peaks to lower temperatures, thus occurring at temperatures lower than 400 °C. And so, we can conclude that doping of titania can facilitate the oxidation of carbonaceous compounds adsorbed onto the catalysts in catalytic testing. In other words, doping of macro-mesoporous titania can favour the possible auto-regeneration of the catalyst at temperatures lower than those seen for titania supports in the literature. Finally, the deposition of carbonaceous compounds can play an important role in the persistent

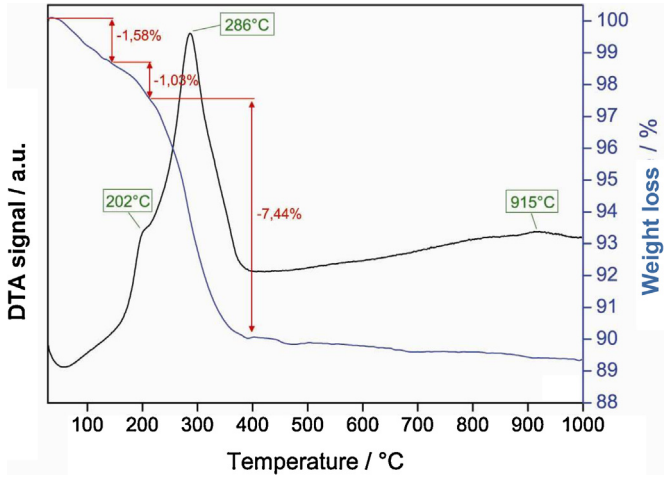

Fig. 10. DTA-TGA profiles of Pd5CeTi catalyst after ageing test.

reduction of PdO particles into metallic Pd, thus verifying results obtained by XRD experiments.

4. Conclusion

The catalytic performance of Ce, Fe and Ni doped macro-mesoporous titania has been investigated in the total oxidation of toluene. Tests show that doping enhanced the catalytic performance of the hierarchically structured titania in terms of activity and selectivity. DR-UV–Visible experiments show the existence of a support-dopant as well as a noble metal–support interaction. Gold loading limited the reduction behaviour of these doped supports and offered a higher performance towards the oxidation of toluene compared to unloaded doped titania. Finally, among the dopants tested, Ce has a significant impact and the efficiency of the doping is in the following order: Ni < Fe < Ce. The dopant content of titania also affects the catalytic performance of doped materials. In fact a high content showed a higher activity towards toluene oxidation with Pd loaded catalysts being much more active than Au loaded ones. Pd5CeTi, being the best performing catalyst, was subjected to an ageing test and showed a stable conversion rate of toluene to CO_2 after 70 h of exposure to a mixture of air and toluene (1000 ppm). DTA-TGA experiments proved the deposition of carbonaceous compounds formed during the catalytic test on the catalyst's surface. Two categories of carbonaceous compounds were noted (light and heavy molecules). However, the experiments also showed that these carbonaceous compounds were oxidized at temperatures lower than 400 °C. This shows that doping and noble metal loading of titania enhances the activity of this support. Furthermore, thanks to the above mentioned result, we are also lead to think that doping could ensure a better and easier regeneration of the catalyst during the removal of VOC molecules.

Acknowledgements

T.T. and V.I. gratefully acknowledge the financial support by the Bulgarian National Science Fund (E 1/7/2012). The authors would also like to thank IRENI and the European Union through an INTERREG IV REDUGAZ project for financial supports.

References

[1] J.J. Spivey, Ind. Eng. Chem. Res. 26 (1987) 2165.
[2] T. Maillet, C. Solleau, J. Barbier Jr., D. Duprez, Appl. Catal. B 14 (1997) 85.
[3] J. Carpentier, J.F. Lamonier, S. Siffert, E.A. Zhilinskaya, A. Aboukaïs, Appl. Catal. A 234 (2002) 91.
[4] M. Ferrandon, E. Björnbom, J. Catal. 200 (2001) 148.
[5] R.W. van den Brink, R. Louw, P. Mulder, Appl. Catal. B 16 (1998) 219.
[6] C. Gennequin, M. Lamallem, R. Cousin, S. Siffert, V. Idakiev, T. Tabakova, A. Aboukaïs, B.L. Su, J. Mater. Sci. 44 (2009) 6654.
[7] T. Barakat, J.C. Rooke, H.L. Tidahy, M. Hosseini, R. Cousin, J.-F. Lamonier, J.-M. Giraudon, G. De Weireld, B.-L. Su, S. Siffert, ChemSusChem 4 (2011) 1420.
[8] J.C. Rooke, T. Barakat, S. Siffert, B.-L. Su, Catal. Today 192 (2012) 183.
[9] K. Okumura, T. Kobayashi, H. Tanaka, M. Niwa, Appl. Catal. B 44 (2003) 325.
[10] S. Scirè, S. Minicò, C. Crisafulli, C. Satriano, A. Pistone, Appl. Catal. B 40 (2003) 43.
[11] M. Hosseini, S. Siffert, H.L. Tidahy, R. Cousin, J.-F. Lamonier, A. Aboukaïs, A. Vantomme, M. Roussel, B.-L. Su, Catal. Today 122 (2007) 391.
[12] V. Idakiev, L. Ilieva, D. Andreeva, J.L. Blin, L. Gigot, B.-L. Su, Appl. Catal. A 243 (2003) 25.
[13] V. Idakiev, T. Tabakova, K. Tenchev, Z.Y. Yuan, T.Z. Ren, A. Vantomme, B.L. Su, J. Mater. Sci. 44 (2009) 6637.
[14] M. Hosseini, H.L. Tidahy, S. Siffert, R. Cousin, A. Aboukaïs, B.-L. Su, Stud. Surf. Sci. Catal. 174 (2008) 1323, Part 2.
[15] T. Machold, W.Y. Suprun, H. Papp, J. Mol. Catal. A: Chem. 280 (2008) 122.
[16] T. Barakat, J.C. Rooke, M. Franco, R. Cousin, J.-F. Lamonier, J.-M. Giraudon, B.-L. Su, S. Siffert, Eur. J. Inorg. Chem. 2012 (2012) 2812.
[17] G.C. Bond, C. Louis, D.T. Thompson, Catalysis by Gold, Imperial College Press, 2006.
[18] D. Andreeva, Gold Bull. 35 (2002) 82.
[19] R. Zanella, L. Delannoy, C. Louis, Appl. Catal. A 291 (2005) 62.
[20] M. Haruta, N. Yamada, T. Kobayashi, S. Iijima, J. Catal. 115 (1989) 301.
[21] S.-J. Lee, A. Gavriilidis, J. Catal. 206 (2002) 305.

[22] M. Lamallem, H.E. Ayadi, C. Gennequin, R. Cousin, S. Siffert, F. Aïssi, A. Aboukaïs, Catal. Today 137 (2008) 367.
[23] P.-O. Larsson, A. Andersson, J. Catal. 179 (1998) 72.
[24] H. Zhu, Z. Qin, W. Shan, W. Shen, J. Wang, J. Catal. 225 (2004) 267.
[25] K. Li, H. Wang, Y. Wei, D. Yan, Chem. Eng. J. 156 (2010) 512.
[26] A.C. Gluhoi, N. Bogdanchikova, B.E. Nieuwenhuys, J. Catal. 232 (2005) 96.
[27] J.-E. Park, T. Momma, T. Osaka, Electrochim. Acta 52 (2007) 5914.
[28] M. Hosseini, T. Barakat, R. Cousin, A. Aboukaïs, B.-L. Su, G. De Weireld, S. Siffert, Appl. Catal. B 111–112 (2012) 218.
[29] R. Abbas-Ghaleb, E. Garbowski, A. Kaddouri, P. Gelin, Catal. Today 117 (2006) 514.
[30] G. Neri, M.G. Musolino, C. Milone, D. Pietropaolo, S. Galvagno, Appl. Catal. A 208 (2001) 307.
[31] K.-I. Fujimoto, F.H. Ribeiro, M. Avalos-Borja, E. Iglesia, J. Catal. 179 (1998) 431.
[32] K. Moljord, P. Magnoux, M. Guisnet, Appl. Catal. A 122 (1995) 21.
[33] K. Moljord, P. Magnoux, M. Guisnet, Appl. Catal. A 121 (1995) 245.
[34] M. Hosseini, S. Siffert, R. Cousin, A. Aboukaïs, Z. Hadj-Sadok, B.-L. Su, C. R. Chim. 12 (2009) 654.
[35] M. Guisnet, P. Magnoux, Appl. Catal. A 212 (2001) 83.
[36] G. Veser, M. Ziauddin, L.D. Schmidt, Catal. Today 47 (1999) 219.
[37] J.G. McCarty, Catal. Today 26 (1995) 283.
[38] P. Dégé, L. Pinard, P. Magnoux, M. Guisnet, Appl. Catal. B 27 (2000) 17.
[39] H.L. Tidahy, S. Siffert, J.-F. Lamonier, R. Cousin, E.A. Zhilinskaya, A. Aboukaïs, B.-L. Su, X. Canet, G. De Weireld, M. Frère, J.-M. Giraudon, G. Leclercq, Appl. Catal. B 70 (2007) 377.
[40] G. Caeiro, J.M. Lopes, P. Magnoux, P. Ayrault, F. Ramôa Ribeiro, J. Catal. 249 (2007) 234.